International Journal of Thermophysics, Vol. 15, No. 3, 1994

n-Hexane as a Model for Compressed Simple Liquids

S. L. Randzio,[1] J.-P. E. Grolier,[2] J. R. Quint,[2] D. J. Eatough,[3] E. A. Lewis,[3] and L. D. Hansen[3]

Received December 13, 1993

Isobaric thermal expansivities, α_p, of *n*-hexane have been measured by pressure-controlled scanning calorimetry from just above the saturation vapor pressure to 40 MPa at temperatures from 303 to 453 K and to 300 MPa at 503 K. These new data are combined with literature data to obtain a correlation equation for α_p valid from 240 to 503 K at pressures up to 700 MPa. Correlation equations are developed for the saturated vapor pressure, specific volume, and isobaric heat capacity of liquid *n*-hexane from 240 to 503 K. Calculated volumes, isobaric and isochoric specific heat capacities, isothermal compressibilities, and thermal coefficients of pressure are presented for the entire range of pressure and temperature. The pressure–temperature behavior of these quantities is discussed as a model behavior for simple liquids without strong intermolecular interactions.

KEY WORDS: *n*-hexane; isobaric thermal expansivities; pressure-controlled scanning calorimetry; saturated vapor pressure; specific volume; heat capacity; isothermal compressibility; thermal coefficient of pressure.

1. INTRODUCTION

In the absence of a quantitative theory for dense molecular fluids, the interpretation of experimental data for liquids over large pressure and temperature ranges could be done by comparison with the behavior of a simple liquid under similar conditions of pressure and temperature [1]. However, no suitable data set exists that can be used to develop or confirm simple liquid models. Such a model is needed to suggest the general rules for

[1] Institute of Physical Chemistry, Polish Academy of Sciences, ul. Kasprzaka 44/52, 01-224 Warsaw, Poland.

[2] Laboratoire de Thermodynamique et Génie Chimique, Université Blaise-Pascal, F-63177 Aubiere Cedex, France.

[3] Department of Chemistry, Brigham Young University, Provo, Utah 84602-1022, U.S.A.

0195-928X/94/0500-0415$07.00/0

describing the properties of simple liquids as functions of pressure and temperature and for the eventual development of a physically based equation of state for dense fluids. The behavior of such properties as the minimum in the isotherm of the isobaric heat capacity, the effect of temperature on the location of this minimum, the intersection point of isotherms of the isobaric thermal expansivity, and the change in shape of volume isobars with increasing pressure have been discussed in the literature [1–4], but all need to be described for much larger temperature and pressure ranges. Further studies should also concentrate on examination of the shape of isobaric heat-capacity isobars at pressures above and below the minimum on the isotherms, and on the behavior of the isochoric heat capacity, coefficient of isothermal compressibility, thermal coefficient of pressure, and the difference between isobaric and isochoric heat capacities, all as functions of pressure and temperature. The aim of the present study is to present results of measurements and calculations of these properties for *n*-hexane over the temperature range from 243.15 to 503.15 K under pressures from the saturation line up to 700 MPa.

n-Hexane has previously been suggested as a model substance [2–4] because of the large amount of literature data available, but an adequate and precise description of several properties including isobaric thermal expansivity, isobaric and isochoric heat capacities, and volume has not yet been reported for sufficiently large pressure and temperature ranges. Grigoryev et al. [5] summarized the Grozny Petroleum Institute's data on *n*-hexane from 180 to 630 K and up to 100 MPa with an equation of state in polynomial form. Unfortunately, the published equation contains typographical errors which have not yet been corrected and the equation is not usable. The best source of data obtained on *n*-hexane by the Grozny Petroleum Institute is therefore a publication by the Russian Committee on Standards [6]. Pruzan published a fitted equation [2] followed by experimental data [4] for the isobaric thermal expansivity of *n*-hexane from 238.6 to 471.8 K and up to 700 MPa. We previously published experimental data on the isobaric thermal expansivity of *n*-hexane from 303 to 503 K and from about 15 to 400 MPa [7]. Both Pruzan's [4] and our data [7] sets lack precise measurements at low pressures because the wide-range pressure sensors used were not precise at low pressures. The imprecision in the data at low pressures over the entire temperature range has prevented accurate determination of the pressure effect on the thermodynamic properties of *n*-hexane over the p, T surface of the liquid phase from the saturation line to high pressures. This paper presents new calorimetric measurements of the isobaric thermal expansion coefficient of *n*-hexane measured from near the vapor pressure saturation line up to about 35 MPa at temperatures from 303.1 to 452.8 K and at 503.1 K under

pressures up to 275.6 MPa. The latter data at higher pressures were collected to augment the literature data set near the critical temperature of 507.8 K.

Calculation of pressure effects on the thermodynamic properties of liquid *n*-hexane requires that reference data be expressed in the form of analytical equations. As part of this study, equations were developed to describe the saturation vapor pressure from 240 to 503 K, the specific volume and isobaric heat capacity of the liquid from 243.15 to 503.15 K along the saturation vapor pressure line, and the specific volume as a function of pressure up to 700 MPa at 298.15 K.

2. EXPERIMENTS

2.1. Instrument and Methods

The instrument used in the present study was constructed at the Laboratoire de Thermodynamique et Génie Chimique at the University Blaise Pascal of Clermont Ferrand in coorperation with the Institute of Physical Chemistry at Warsaw. The instrument is similar to that described previously [7], except the calorimetric cells have been modified to reduce heat transfer out of the calorimeter and the pressure programming system has been fully automated.

A diagram of the calorimetric vessel is shown in Fig. 1. The calorimetric vessels are mounted differentially and are made from 4.76-mm-i.d., type 304 stainless-steel tubing. The vessels are connected through a high-pressure reducer inside the calorimeter thermostat to a capillary tube (type 316 stainless steel, 6.35-mm o.d., 1.59-mm i.d.). The capillary connects the calorimetric vessel to the pressure generating system.

The Bourdon tube high-pressure gauge used in an earlier instrument [7] was replaced by an extensiometric pressure detector made and calibrated from 0.1 to 500 MPa against a free-piston deadweight pressure balance at the Institute of Physics of the Technical University at Warsaw. The extensiometric detector was used over the entire range for automation purposes and to measure pressures above 40 MPa. A digital pressure gauge (Heise Model 710) was used to measure pressures below 40 MPa. To avoid damaging the Heise gauge when the system pressure was above 40 MPa, the Heise gauge was isolated by a valve. The uncertainty in pressure measurements made with these two instruments is estimated to be ± 0.01 MPa or $\pm 0.1\%$, whichever is greater.

The calorimeter temperature was calibrated with a platinum resistance thermometer placed inside the calorimetric cell during calibration. The

uncertainty in temperature measurements is estimated to be less than 0.1 K. A more detailed description of the instrument will be presented elsewhere.

The calorimeter system was calibrated with nitrogen at 303, 353, 403, 453, and 503 K [7]. The standard deviation of the mean of the calibration constant was about 1.4% at each temperature.

Measurements on *n*-hexane were made as previously described [7]. Thermal expansivities, α_p, were calculated from Eq. (1):

$$\alpha_p - \alpha_{p,ss} = -kI/(T\,\Delta p) \tag{1}$$

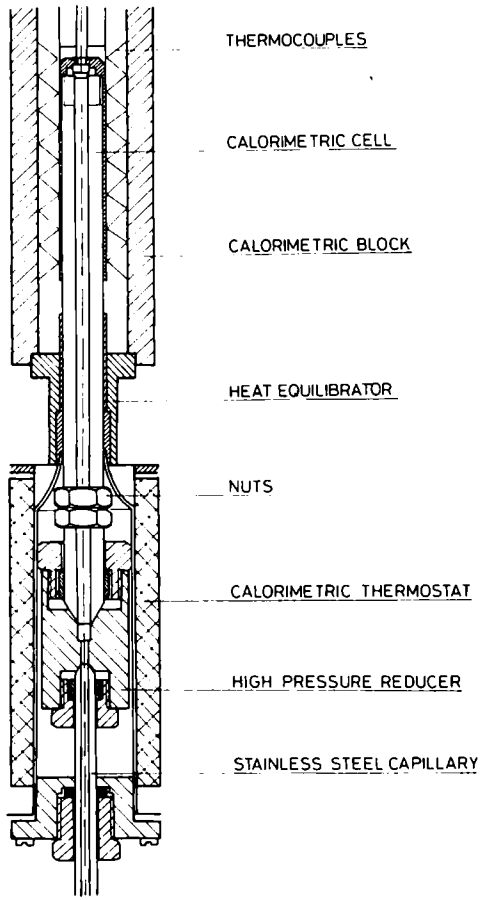

Fig. 1. Schematic diagram of the calorimetric cell.

where k is the calibration constant obtained with nitrogen, I is the integral of the calorimetric signal (heat rate) over time from the response to a pressure step Δp, and $\alpha_{p,ss}$ is the thermal expansivity of stainless steel ($5.1 \times 10^{-5}\ K^{-1}$). The error of determination of integral I never exceeded 0.2%. Taking into account the errors made on determination of all parameters of Eq. (1), the error of determination of thermal expansivities in this study is estimated to be less than 2%.

2.2. Materials

Nitrogen was 99.995% obtained from Alphagaz, France, with the following stated impurities: <5 ppmv oxygen, <3 ppmv water, and <1.5 ppmv hydrocarbons. *n*-Hexane was 99.5% (Fluka 52765) and was used without further purification.

3. RESULTS

3.1. The Isobaric Coefficient of Thermal Expansion

The results of the measurements made in this study are presented in Table I. Pressure values given in Table I are the mean values between the beginning and the end of a pressure step, Δp. The end values were measured at the end of the thermogram, after thermal and mechanical equilibrium were established. Each ending pressure became the beginning pressure for the next step. Measurements were made with decreasing pressure. After initial pressurization to the highest pressure, the system was allowed to equilibrate thermally and mechanically for a few hours before measurements began.

The experimental results in Table I, data published in our previous paper [7], and the experimental results of Pruzan [4] were fitted by least squares to Eq. (2)

$$\alpha_p(p, T) = [a(T)][p - p_s + b(T)]^{-0.5} \tag{2}$$

where p is pressure in MPa, p_s is the saturation vapor pressure, and $a(T)$ and $b(T)$ are functions of temperature. The saturation vapor pressure must also be accurately known because it is the lower limit used for integrations to obtain other thermodynamic functions.

Equation (3) for the saturation vapor pressure in MPa as a function of the absolute temperature in kelvins, T, was obtained from least-squares fit of selected literature data [8–14], altogether 264 data points.

$$p_s = \exp(a_0 + a_1 T^{-1} + a_2 T + a_3 T^2) \tag{3}$$

Values for the coefficients are given in Table II. The equation proposed by Pruzan [4] does not fit the p_s data accurately, probably because of typographical errors in the publication. The standard deviation of the differences between the calculated, Eq. (3), and the experimental data is 0.59% and the average deviation is −0.03% from 240 K to the critical

Table I. Pressure-Controlled Scanning Calorimetric Measurements of Isobaric Thermal Expansivities of *n*-Hexane

T (K)	Δp (MPa)[a]	p (MPa)	α_p (10^{-3} K^{-1})
303.1	1.62	0.87	1.419
303.1	2.55	2.95	1.380
303.1	2.42	5.43	1.371
303.1	4.86	9.04	1.315
303.1	9.80	16.39	1.204
303.1	10.03	26.31	1.132
303.1	9.25	35.92	1.056
352.6	2.37	2.37	1.666
352.6	5.17	6.14	1.516
352.6	6.97	12.21	1.390
352.6	9.90	20.64	1.253
402.6	2.16	2.68	2.048
402.6	5.09	6.30	1.843
402.6	3.92	10.80	1.657
402.6	6.15	15.83	1.450
402.6	9.82	23.82	1.302
452.8	3.30	3.13	3.124
452.8	4.07	6.82	2.356
452.8	6.05	11.88	1.922
452.8	8.64	19.22	1.586
452.8	10.18	28.63	1.320
503.1	0.895	4.68	5.523
503.1	2.22	6.23	4.129
503.1	5.02	10.40	2.646
503.1	7.67	23.97	1.563
503.1	14.91	42.55	1.129
503.1	28.93	64.5	0.914
503.1	21.02	89.4	0.757
503.1	22.02	111.0	0.689
503.1	23.00	133.5	0.622
503.1	34.62	162.3	0.570
503.1	24.00	191.6	0.514
503.1	35.29	221.2	0.479
503.1	24.51	251.3	0.454
503.1	23.99	275.6	0.448

[a] See Eq. (1).

Table II. Values of Coefficients in Eqs. (3)–(5), (7), and (14)

Eq. No.	Coefficient								
	a_0	a_1	a_2	a_3	a_4	a_5	a_6	a_7	a_8
(3)	20.319604	−5234.93	$-2.9230897 \times 10^{-2}$	2.30413×10^{-5}					
(4)	7.117×10^{-3}	-2.482456×10^{-6}	4.01821×10^{-8}	3.207×10^{-3}					
(5)	-2.344×10^{-2}	1.29388×10^{-3}	5.76483×10^{-6}	1.97294×10^{-8}	2.952×10^{-2}				
(7)	3.54133	-1.76928×10^{-2}	-5.1278×10^{-5}	-1.659349×10^{-7}	$-3.476782 \times 10^{-10}$	$-3.295608 \times 10^{-13}$	0.73867	−0.30811	
(14)	63.653982	−112.126374	83.741181	−32.989161	7.2536755	−0.84439977	0.040708181	−5.3019296	−6.1225693

point. The points appear to be randomly distributed around the calculated line. With respect to the equation reported in Ref. 6, our calculated values are lower by an average deviation of 0.47% from 243.15 K to the critical point.

Once p_s was known, $a(T)$ and $b(T)$ were obtained from a least-squares fit of the $\alpha_p(p, T)$ data (in K^{-1}) as shown in Eqs. (4)–(6),

$$a(T) = a_0 + a_1 h + a_2 h^2 + a_3 \exp(h) \tag{4}$$

$$b(T) = a_0 h + a_1 h^2 + a_2 h^3 + a_3 h^4 + a_4 \exp(h) \tag{5}$$

$$h = T - T_c \tag{6}$$

where T_c is the critical temperature, 507.8 K. Values of coefficients are given in Table II.

A plot of the thermal expansivities obtained with Eqs. (2)–(6) is given in Fig. 2. The standard deviation of the differences between the calculated and the experimental data over the whole temperature and pressure surface, without elimination of any of 392 available experimental data points, is 3.6% and the average deviation is −0.09%. The points appear to be randomly distributed around the calculated isotherms. At pressures above 70 MPa, the equations agree within the standard deviation of the

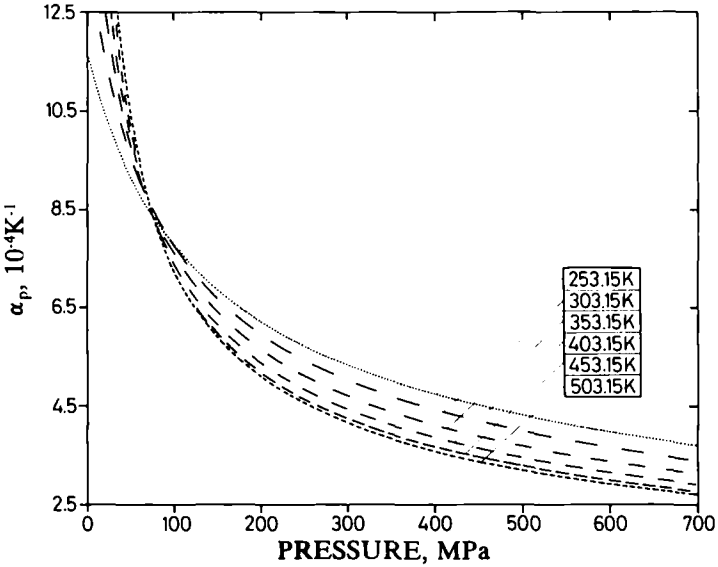

Fig. 2. Isobaric thermal expansivities (α_p) of *n*-hexane calculated with Eqs. (2)–(6).

experimental data with the equation given by Pruzan [2], however, at pressures below 70 MPa, large differences occur. The difference increases as the temperature increases, and above 487.35 K the equation of Pruzan [2] becomes meaningless because the expression under the square root becomes negative.

To verify the thermal expansivities of liquid *n*-hexane obtained with Eqs. (2)–(6) along the vapor pressure saturation line, or at atmospheric pressure at low temperatures, a comparison was made with thermal expansivities calculated from volumetric data reported in the literature. The literature data on the volume of liquid *n*-hexane under saturation pressure [8, 9, 15–17] were fitted to Eq. (7)

$$v(p_s, T) = a_0 + h\big(a_1 + h\{a_2 + h[a_3 + h(a_4 + a_5 h)]\}\big) + a_6 \exp(h) + a_7 \mathrm{sqrt}(h) \tag{7}$$

with the coefficients given in Table II and $h = T - T_c$, where $T_c = 507.8$ K. The average deviation between the calculated values and the experimental data points is +0.02% and the standard deviation is 0.27% from 240.15 to 503.15 K, the largest deviation being 1.2% at 503.15 K with data from Ref. 8. Thermal expansivities of the liquid *n*-hexane under saturation were calculated from Eq. (7) and compared with the values obtained from Eqs. (2)–(6). The average deviation over the entire temperature range is +1.4% and the standard deviation of the differences is 2.9%. The largest deviations are at temperatures below 300 K, where the values obtained with Eqs. (2)–(6) are lower by about 5% than the values obtained from the saturation volume equation.

Very good agreement was also found with thermal expansivities calculated from densities reported in Ref. 6, where along the 100 MPa isobar at temperatures from 250 to 500 K, the values from Eqs. (2)–(6) are on average lower by 2% but are within the experimental error. Accurate volumetric measurements at pressures above 100 MPa are difficult, and expansivities obtained from reported data [18–22] are scattered. For example, thermal expansivities calculated from data in Ref. 21, where the data are reported for rather large temperature and pressure ranges, deviate with respect to values from Eqs. (2)–(6) by −1 to +8% along the 300-MPa isobar over the temperature range from 298.15 to 473.15 K and by −2.9 to +9% along the 500-MPa isobar over the same temperature range.

3.2. Volume

The specific volumes of liquid *n*-hexane from the saturation line up to 700 MPa and from 243.15 to 503.15 K have been calculated with Eq. (8).

Table III. Specific Volume ($1000 \times m^3 \cdot kg^{-1}$) of *n*-Hexane Calculated with Eq. (8)

	p (MPa)												
T (K)	100	120	140	160	180	200	250	300	350	400	500	600	700
243.15	1.3259	1.3129	1.3010	1.2902	1.2802	1.2709	1.2502	1.2323	1.2165	1.2024	1.1780	1.1574	1.1395
263.15	1.3467	1.3324	1.3194	1.3076	1.2968	1.2868	1.2645	1.2455	1.2287	1.2139	1.1882	1.1666	1.1480
283.15	1.3678	1.3521	1.3380	1.3251	1.3134	1.3026	1.2788	1.2585	1.2408	1.2251	1.1982	1.1757	1.1563
298.15	1.3844	1.3675	1.3524	1.3388	1.3264	1.3150	1.2899	1.2687	1.2502	1.2339	1.2060	1.1828	1.1628
303.15	1.3892	1.3720	1.3565	1.3427	1.3300	1.3184	1.2929	1.2714	1.2527	1.2361	1.2080	1.1845	1.1643
323.15	1.4109	1.3919	1.3752	1.3601	1.3465	1.3340	1.3069	1.2840	1.2643	1.2469	1.2175	1.1930	1.1722
343.15	1.4327	1.4119	1.3937	1.3775	1.3628	1.3495	1.3206	1.2965	1.2757	1.2575	1.2268	1.2014	1.1798
363.15	1.4546	1.4320	1.4122	1.3948	1.3791	1.3648	1.3342	1.3087	1.2869	1.2679	1.2359	1.2096	1.1872
383.15	1.4766	1.4520	1.4307	1.4119	1.3952	1.3800	1.3476	1.3207	1.2979	1.2781	1.2448	1.2176	1.1945
403.15	1.4987	1.4720	1.4491	1.4290	1.4111	1.3951	1.3608	1.3326	1.3088	1.2881	1.2535	1.2254	1.2016
423.15	1.5209	1.4921	1.4675	1.4460	1.4270	1.4100	1.3739	1.3444	1.3194	1.2979	1.2621	1.2331	1.2086
443.15	1.5432	1.5122	1.4859	1.4630	1.4429	1.4249	1.3868	1.3560	1.3300	1.3077	1.2706	1.2406	1.2155
463.15	1.5658	1.5324	1.5043	1.4800	1.4587	1.4397	1.3998	1.3675	1.3405	1.3173	1.2790	1.2481	1.2222
483.15	1.5887	1.5528	1.5228	1.4970	1.4745	1.4545	1.4127	1.3790	1.3509	1.3269	1.2873	1.2555	1.2290
493.15	1.6002	1.5631	1.5321	1.5056	1.4824	1.4619	1.4191	1.3847	1.3561	1.3317	1.2914	1.2592	1.2323
500.15	1.6083	1.5703	1.5387	1.5116	1.4880	1.4671	1.4236	1.3888	1.3598	1.3350	1.2943	1.2618	1.2346
503.15	1.6118	1.5734	1.5415	1.5142	1.4904	1.4694	1.4256	1.3905	1.3613	1.3364	1.2956	1.2629	1.2356

Thermal expansivity data were obtained from Eqs. (2)–(6) and the specific reference volume isotherm at $T_R = 298.15$ K.

$$v(p, T) = v(T_R, p) \exp\left[\int_{T_R}^{T} \alpha_p \, dT\right] \tag{8}$$

The specific reference volume isotherm $v(T_R, p)$ in $cm^3 g^{-1}$ was obtained by fitting literature data [16, 21, 22] to Eq. (9).

$$v(T_R, p) = v_0\{1 - C \ln[(B + p)/(B + 0.1013)]\} \tag{9}$$

where pressure is in MPa, $B = 56.9$, $C = 0.092226$, and $v_0 = 1.5264$. The standard deviation of the differences between the experimental data and Eq. (9) is 0.12%, and the average deviation is +0.007%. Although the experimental data go up to only 533.8 MPa, Eq. (9) is a form of the Tait equation [23] which has physically meaningful coefficients [24], and thus the calculated values of the reference volume are probably correct up to at least 700 MPa. The results of calculations of the specific volume with Eq. (8) for pressures from 100 to 700 MPa at temperatures from 243.15 to 503.15 K are given in Table III. Data sets reported in the literature [6, 16–22] for lower pressures and this temperature range appear to be accurate within a few tenths of a percent.

3.3. Coefficient of Isothermal Compressibility

The isothermal compressibilities, κ, were calculated with a form of the Tait equation, Eq. (10), at selected temperatures from 243.15 to 503.15 K at pressures from the saturation line up to 700 MPa.

$$\kappa_T = C/\left((B + p)\{1 - C \ln[(B + p)/(B + p_s)]\}\right) \tag{10}$$

Table IV gives the values of the coefficients B and C obtained by fitting volume data from Eq. (8) and p_s data from Eq. (3) at each temperature. Table IV also gives standard and average deviations of the differences between the specific volumes obtained with the Tait equation and the volumes calculated with Eqs. (8) and (9). The agreement is very good (SD < 0.15%) up to about 493 K but becomes poorer (0.15% < SD < 0.45%) at higher temperatures and, particularly, as the critical temperature (507.8 K) is approached. Figure 3 presents isotherms of the isothermal coefficient of compressibility calculated with Eq. (10). The isotherms of the coefficient of compressibility do not demonstrate an intersection point as do the isotherms of isobaric thermal expansivity given in Fig. 2.

Table IV. Coefficients B and C of the Tait Equation for n-Hexane

T (K)	B (MPa)	C (10^{-3})	SD (%)	Average deviation (%)
243.15	107.390	97.797	0.15	0.060
263.15	85.1088	95.139	0.09	0.085
283.15	67.5381	93.216	0.03	0.010
303.15	53.6496	91.917	0.01	−0.003
323.15	42.7768	91.201	0.03	−0.009
343.15	33.8653	90.732	0.04	−0.009
363.15	26.2836	90.248	0.05	−0.011
383.15	19.8444	89.741	0.05	−0.006
403.15	14.2878	88.980	0.07	−0.004
423.15	9.52198	87.816	0.09	−0.003
443.15	5.37777	86.036	0.14	−0.002
463.15	1.92352	83.267	0.21	−0.003
483.15	−0.81138	78.508	0.30	−0.004
493.15	−1.87445	74.616	0.36	−0.001
500.15	−2.48261	70.756	0.41	0.003
503.15	−2.71150	67.838	0.45	0.002

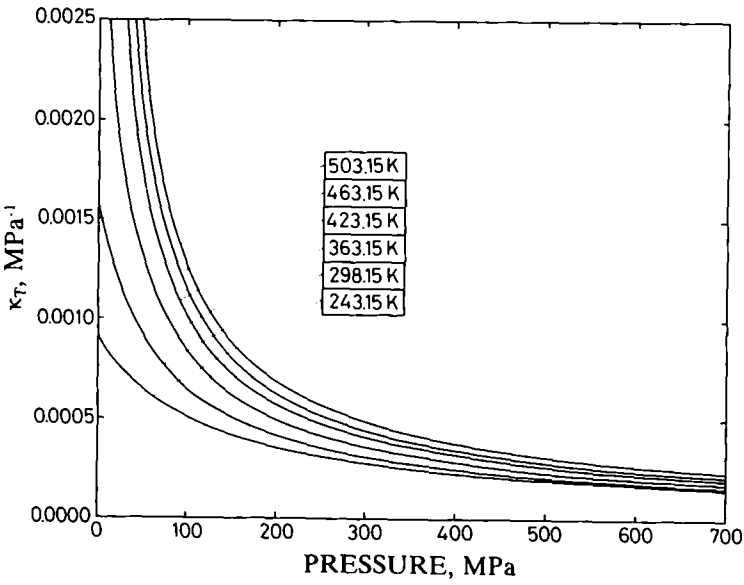

Fig. 3. Isothermal compressibilities (κ_T) of n-hexane calculated with Eq. (10).

3.4. Thermal Coefficient of Pressure

The thermal coefficient of pressure, $(\partial p/\partial T)_v$, of liquid *n*-hexane at selected temperatures from 243.15 to 503.15 K at pressures from the saturation line up to 700 MPa was calculated from Eq. (11) (Fig. 4).

$$(\partial p/\partial T)_v = \alpha_p/\kappa_T \tag{11}$$

A graphic presentation of selected isotherms is given in Fig. 4. Numerical values for $(\partial p/\partial T)_v$ can be obtained from values for α_p from Eqs. (2)–(6) and values for κ_T from Eq. (10).

3.5. Isobaric Heat Capacity

The effects of pressure on the isobaric heat capacity of liquid *n*-hexane at selected temperatures were calculated with Eq. (12).

$$\Delta^p_{p_s} C_{p,T}(p) = -T \int_{p_s}^{p} v(p, T)[\alpha_p^2 + (\partial \alpha_p/\partial T)_p]\, dp \tag{12}$$

$v(p, T)$ values were calculated with Eqs. (8) and (9), α_p values with Eqs. (2)–(6), and $\partial \alpha_p/\partial T$ values with the derivative of Eqs. (2)–(6). $\Delta^p_{p_s} C_{p,T}(p)$

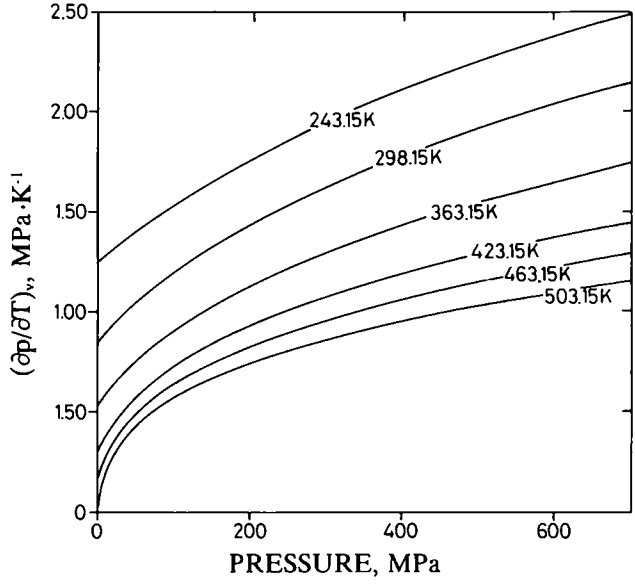

Fig. 4. Thermal coefficient of pressure $(\partial p/\partial T)_v$ of *n*-hexane calculated with Eq. (11).

Table V. Pressure Effects on Isobaric Specific Heat Capacity of *n*-Hexane, $\Delta_{p_1}^{p} C_{p,T}(p)$ in $kJ \cdot K^{-1} \cdot kg^{-1}$

p	T(K)															
(MPa)	243.15	263.15	283.15	298.15	303.15	323.15	343.15	363.15	383.15	403.15	423.15	443.15	463.15	483.15	493.15	500.15	503.15
5	−0.008	−0.010	−0.012	−0.014	−0.015	−0.018	−0.023	−0.029	−0.038	−0.052	−0.075	−0.116	−0.197	−0.402	−0.673	−1.161	−1.699
10	−0.015	−0.019	−0.023	−0.026	−0.027	−0.033	−0.041	−0.051	−0.066	−0.089	−0.125	−0.187	−0.303	−0.564	−0.872	−1.388	−1.940
15	−0.022	−0.027	−0.032	−0.036	−0.038	−0.045	−0.054	−0.067	−0.086	−0.113	−0.157	−0.228	−0.355	−0.629	−0.942	−1.461	−2.012
20	−0.028	−0.033	−0.039	−0.044	−0.046	−0.055	−0.066	−0.080	−0.101	−0.131	−0.178	−0.254	−0.388	−0.666	−0.981	−1.499	−2.051
25	−0.034	−0.040	−0.046	−0.052	−0.054	−0.063	−0.075	−0.090	−0.112	−0.144	−0.194	−0.273	−0.410	−0.691	−1.006	−1.524	−2.076
30	−0.038	−0.045	−0.052	−0.058	−0.060	−0.070	−0.082	−0.098	−0.121	−0.155	−0.206	−0.287	−0.426	−0.709	−1.024	−1.542	−2.093
35	−0.043	−0.050	−0.057	−0.064	−0.066	−0.076	−0.088	−0.105	−0.128	−0.163	−0.216	−0.298	−0.438	−0.722	−1.038	−1.556	−2.107
40	−0.047	−0.054	−0.062	−0.068	−0.071	−0.080	−0.093	−0.110	−0.134	−0.170	−0.223	−0.307	−0.448	−0.733	−1.049	−1.567	−2.118
50	−0.054	−0.062	−0.070	−0.076	−0.078	−0.088	−0.101	−0.118	−0.143	−0.179	−0.234	−0.320	−0.463	−0.749	−1.065	−1.583	−2.134
60	−0.060	−0.068	−0.076	−0.082	−0.084	−0.094	−0.107	−0.124	−0.149	−0.186	−0.242	−0.329	−0.473	−0.760	−1.076	−1.594	−2.145
70	−0.065	−0.073	−0.081	−0.087	−0.089	−0.098	−0.111	−0.128	−0.153	−0.191	−0.248	−0.335	−0.480	−0.768	−1.085	−1.603	−2.154
80	−0.069	−0.077	−0.084	−0.090	−0.092	−0.101	−0.114	−0.131	−0.156	−0.194	−0.252	−0.340	−0.486	−0.775	−1.091	−1.610	−2.161
90	−0.073	−0.080	−0.087	−0.093	−0.095	−0.104	−0.116	−0.133	−0.158	−0.196	−0.254	−0.344	−0.490	−0.780	−1.097	−1.615	−2.166
100	−0.076	−0.083	−0.090	−0.095	−0.097	−0.105	−0.117	−0.134	−0.159	−0.198	−0.256	−0.346	−0.494	−0.784	−1.101	−1.620	−2.171
120	−0.081	−0.087	−0.093	−0.097	−0.099	−0.107	−0.118	−0.134	−0.160	−0.199	−0.259	−0.350	−0.499	−0.790	−1.108	−1.627	−2.178
140	−0.084	−0.089	−0.095	−0.098	−0.100	−0.107	−0.117	−0.134	−0.160	−0.199	−0.259	−0.351	−0.501	−0.794	−1.112	−1.632	−2.183
160	−0.086	−0.091	−0.095	−0.098	−0.099	−0.106	−0.116	−0.132	−0.158	−0.198	−0.259	−0.352	−0.503	−0.797	−1.116	−1.636	−2.187
180	−0.087	−0.091	−0.095	−0.097	−0.098	−0.104	−0.114	−0.130	−0.156	−0.197	−0.258	−0.352	−0.504	−0.799	−1.119	−1.639	−2.190
200	−0.088	−0.091	−0.094	−0.096	−0.097	−0.102	−0.111	−0.127	−0.154	−0.194	−0.257	−0.351	−0.505	−0.801	−1.121	−1.641	−2.193
250	−0.087	−0.088	−0.089	−0.090	−0.091	−0.095	−0.104	−0.120	−0.146	−0.188	−0.252	−0.348	−0.504	−0.802	−1.124	−1.645	−2.197
300	−0.084	−0.084	−0.083	−0.083	−0.084	−0.087	−0.095	−0.111	−0.138	−0.181	−0.246	−0.344	−0.502	−0.803	−1.125	−1.647	−2.200
350	−0.079	−0.078	−0.076	−0.076	−0.076	−0.078	−0.086	−0.102	−0.130	−0.174	−0.240	−0.340	−0.499	−0.802	−1.126	−1.649	−2.202
400	−0.074	−0.072	−0.069	−0.067	−0.067	−0.069	−0.077	−0.093	−0.121	−0.166	−0.233	−0.335	−0.496	−0.801	−1.125	−1.649	−2.202
500	−0.063	−0.058	−0.053	−0.051	−0.050	−0.051	−0.059	−0.076	−0.105	−0.151	−0.221	−0.325	−0.489	−0.797	−1.124	−1.649	−2.203
600	−0.050	−0.043	−0.037	−0.034	−0.033	−0.034	−0.041	−0.059	−0.089	−0.136	−0.208	−0.315	−0.482	−0.793	−1.122	−1.648	−2.203
700	−0.037	−0.029	−0.021	−0.017	−0.017	−0.017	−0.025	−0.042	−0.073	−0.123	−0.196	−0.305	−0.475	−0.789	−1.119	−1.646	−2.201

values were then obtained by numerical integration. The results of the calculations are given in Table V. Isotherms of $\Delta^{p}_{p_s} C_{p,T}(p)$ are presented in Fig. 5. The isotherms of $\Delta^{p}_{p_s} C_{p,T}(p)$ do not cross and the minimum is shifted to higher pressures as the temperature increases.

The isobaric heat capacity of liquid *n*-hexane as a function of p and T can be calculated with the thermodynamic relation in Eq. (13),

$$C^{l}_{p}(p, T) = C^{l}_{p,p_s} + \Delta^{p}_{p_s} C^{l}_{p}(p, T) \tag{13}$$

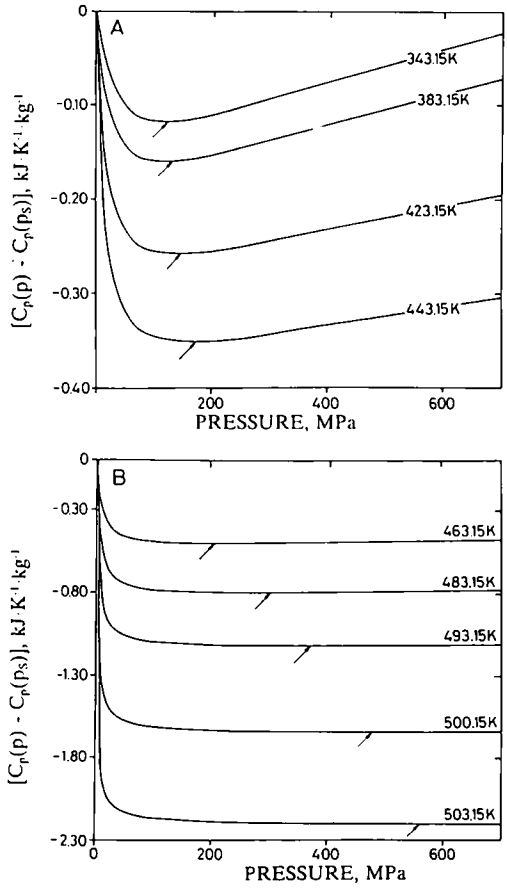

Fig. 5. Pressure effect on the specific isobaric heat capacity (C_p) of liquid *n*-hexane as a function of pressure over the middle-temperature range (A) and the high-temperature range (B). The arrows show the location of the minima in the curves.

Table VI. Isochoric Specific Heat Capacity ($kJ \cdot K^{-1} \cdot kg^{-1}$) of *n*-Hexane

p	T(K)																
(MPa)	243.15	263.15	283.15	298.15	303.15	323.15	343.15	363.15	383.15	403.15	423.15	443.15	463.15	483.15	493.15	500.15	503.15
p_s	1.598	1.651	1.711	1.759	1.776	1.844	1.915	1.994	2.081	2.178	2.286	2.417	2.590	2.875	3.164	3.607	4.056
5	1.597	1.651	1.713	1.762	1.779	1.849	1.922	2.001	2.088	2.180	2.277	2.385	2.499	2.614	2.664	2.684	2.685
10	1.599	1.654	1.716	1.765	1.782	1.853	1.927	2.006	2.092	2.180	2.271	2.364	2.455	2.531	2.559	2.571	2.571
15	1.600	1.655	1.718	1.767	1.786	1.856	1.931	2.012	2.096	2.183	2.270	2.356	2.439	2.509	2.537	2.552	2.554
20	1.602	1.657	1.720	1.770	1.788	1.860	1.935	2.016	2.100	2.185	2.270	2.354	2.433	2.501	2.530	2.547	2.552
25	1.603	1.659	1.722	1.773	1.791	1.863	1.940	2.020	2.104	2.188	2.272	2.353	2.430	2.498	2.529	2.547	2.553
30	1.604	1.661	1.724	1.776	1.793	1.867	1.944	2.025	2.108	2.191	2.274	2.354	2.430	2.498	2.529	2.549	2.556
35	1.606	1.663	1.727	1.778	1.797	1.870	1.948	2.028	2.112	2.194	2.276	2.355	2.431	2.499	2.531	2.552	2.559
40	1.608	1.664	1.729	1.780	1.799	1.873	1.951	2.032	2.116	2.199	2.279	2.357	2.433	2.501	2.534	2.555	2.562
50	1.611	1.668	1.733	1.786	1.805	1.880	1.959	2.040	2.123	2.205	2.285	2.363	2.437	2.506	2.539	2.561	2.569
60	1.614	1.672	1.738	1.791	1.810	1.886	1.966	2.048	2.131	2.212	2.292	2.368	2.442	2.511	2.545	2.567	2.575
70	1.617	1.675	1.743	1.797	1.816	1.893	1.973	2.054	2.138	2.219	2.298	2.374	2.448	2.515	2.549	2.572	2.581
80	1.620	1.679	1.747	1.802	1.821	1.899	1.979	2.061	2.145	2.226	2.304	2.380	2.452	2.521	2.555	2.578	2.586
90	1.624	1.683	1.751	1.807	1.825	1.905	1.986	2.068	2.152	2.233	2.311	2.386	2.458	2.525	2.559	2.583	2.592
100	1.627	1.687	1.757	1.811	1.831	1.910	1.991	2.074	2.158	2.239	2.316	2.391	2.462	2.530	2.564	2.587	2.596
120	1.634	1.695	1.764	1.821	1.841	1.922	2.004	2.087	2.170	2.250	2.327	2.401	2.471	2.538	2.573	2.595	2.604
140	1.640	1.702	1.774	1.831	1.850	1.932	2.016	2.098	2.182	2.262	2.338	2.410	2.481	2.546	2.581	2.603	2.612
160	1.647	1.710	1.782	1.840	1.861	1.942	2.026	2.110	2.193	2.272	2.348	2.420	2.488	2.554	2.588	2.609	2.618
180	1.653	1.717	1.790	1.849	1.869	1.952	2.036	2.120	2.202	2.282	2.357	2.428	2.496	2.561	2.593	2.616	2.624
200	1.659	1.724	1.799	1.857	1.878	1.962	2.045	2.130	2.213	2.291	2.366	2.436	2.503	2.567	2.599	2.621	2.630
250	1.674	1.741	1.818	1.878	1.898	1.983	2.068	2.152	2.235	2.312	2.386	2.454	2.519	2.581	2.612	2.633	2.642
300	1.689	1.757	1.835	1.897	1.917	2.003	2.089	2.173	2.254	2.331	2.403	2.470	2.533	2.594	2.624	2.644	2.653
350	1.702	1.773	1.852	1.915	1.936	2.022	2.108	2.191	2.272	2.349	2.420	2.486	2.547	2.605	2.633	2.653	2.662
400	1.716	1.788	1.868	1.931	1.952	2.040	2.125	2.210	2.290	2.365	2.434	2.499	2.558	2.615	2.643	2.662	2.670
500	1.742	1.817	1.898	1.963	1.984	2.072	2.158	2.241	2.321	2.394	2.461	2.522	2.579	2.633	2.658	2.676	2.683
600	1.765	1.843	1.926	1.989	2.013	2.100	2.186	2.269	2.348	2.419	2.485	2.543	2.598	2.647	2.672	2.689	2.696
700	1.789	1.867	1.951	2.016	2.038	2.127	2.212	2.294	2.372	2.442	2.506	2.563	2.614	2.661	2.684	2.700	2.706

where C^{l}_{p,p_s} is the isobaric heat capacity of liquid *n*-hexane at the pressure of the saturated vapor. Data for C^{l}_{p,p_s} were obtained for the temperature range from 240 to 423 K from the correlation equation of Ruzicka et al. [25], which is based on calorimetric data from the literature and from Gerasimov's [47] heat capacities measured with a flow calorimeter at 5.002 MPa from 350 to 503 K. The isobaric heat capacity data of Gerasimov [47] were reduced to the saturated vapor pressure with Eq. (12). The uncertainty in this correction is only 1 to 2% and the correction is small over most of the temperature range, increasing from about 1% at 350 K to about 5% at 450 K and then up to about 20% at 500 K. $C^{l}_{p,p_s}(T)$ data were fitted by least squares to Eq. (14).

$$C^{l}_{p,p_s}(T) = a_0 + g\{a_1 + g(a_2 + g\{a_3 + g[a_4 + g(a_5 + a_6 g)]\})\} + a_7/k + a_8 \exp(k) \tag{14}$$

where $g = T/100$, $k = T - 507$ [we note that 507.8 does not fit the data properly in Eq. (14)] and the coefficients a_0–a_7 are given in Table II. The standard deviation of the difference between the values obtained from Eq. (14) and the values derived from the correlation equation of Ruzicka et al. [25] and the experimental points of Gerasimov [47] corrected for the pressure effect is 0.77% and the average difference is +0.07%.

3.6. Isochoric Heat Capacity

The isochoric heat capacity at selected temperatures as a function of pressure up to 700 MPa was calculated with Eq. (15).

$$C_v = C_p - Tv\alpha_p^2/\kappa_T \tag{15}$$

Values for C_p were calculated from data in Table V and Eqs. (13) and (14), values for v were from Table IV as calculated with Eqs. (8) and (9), values for α_p were calculated with Eqs. (2)–(6), and values for κ_T with Eq. (10).

The results of calculations of C_v are presented in Table VI. It is interesting to note that the isochoric heat capacity continuously increases with pressure below 403 K, but above 403 K it demonstrates a minimum similar to that of the C_p isotherms. Isotherms showing the influence of pressure on the isochoric heat capacity calculated as a difference $C_v(p) - C_v(p_s)$ at selected temperatures are shown in Fig. 6.

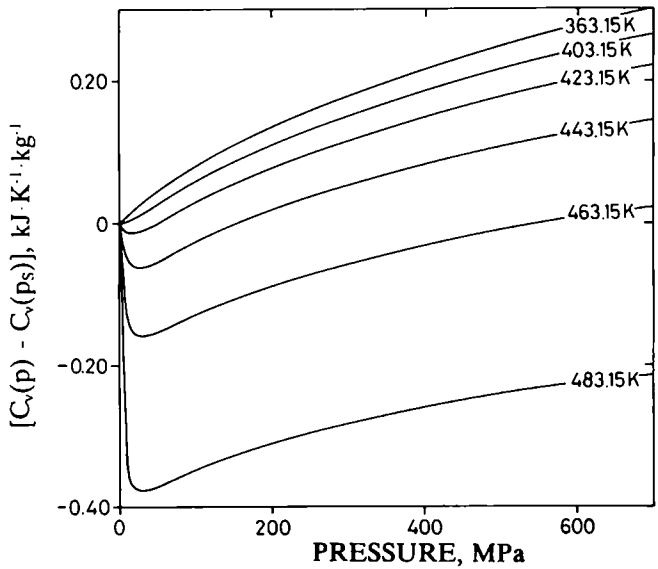

Fig. 6. Pressure effect on the specific isochoric heat capacity (C_v) of liquid *n*-hexane as a function of pressure at selected temperatures.

4. DISCUSSION

The results of measurements and computations on the thermodynamic properties of *n*-hexane presented above significantly exceed the pressure and temperature ranges of previously published data. Direct measurement of isobaric thermal expansivity, the second derivative of the thermodynamic potential, over large pressure and temperature ranges permits accurate calculation by integration of related thermodynamic properties. Because of error propagation in taking derivatives, such results cannot be obtained with volumetric techniques.

The behavior of isobaric thermal expansivity as a function of both pressure and temperature (Fig. 2) is interesting mostly because of the unique crossing point in the isotherms. All except the lowest termperature isotherm, which has a tendency to cross at higher pressures, cross at 65 ± 2 MPa. The behavior of the lowest temperature isotherm may be caused by a change in the structure of the liquid. At the pressure of the crossing point, α_p is independent of temperature. At pressures below (65 ± 2) MPa, α_p increases with temperature, but at higher pressures α_p decreases with temperature. Although no exact theoretical models exist in the literature to explain this behavior, an attempt to explain it has been made by assuming that a molecule in a dense liquid is confined by its

closest neighbors and that the potential well in which the molecule oscillates changes shape with pressure [48].

As a consequence of the crossing of α_p isotherms, the shape of specific volume isobars is different at low and high pressures. This volume behavior is demonstrated in Fig. 7, which shows that the second derivative of specific volume with temperature is positive over the whole temperature range at low pressures but negative at high pressures. Thus the specific volume isobars are concave at low pressures but convex at high pressures. However, it is only the rate of change that increases or decreases with temperature, depending on whether the pressure is high or low. The specific volume itself always increases with temperature over the whole range of pressure and temperature. This study shows that a previous suggestion that the specific volume decreases with temperature above 420 K at certain pressures [4] is incorrect. The error occurred because an inaccurate equation for specific volume was used. Accurate description of the volume isotherms with the Tait equation over the whole temperature and pressure surface is possible only if both the B and the C parameters in Eq. (9) are allowed to vary with temperature. The temperature dependences of these parameters are shown in Fig. 8.

The behavior of both α_p and v determine the pressure effect on the isobaric heat capacity as expressed in the thermodynamic relation in

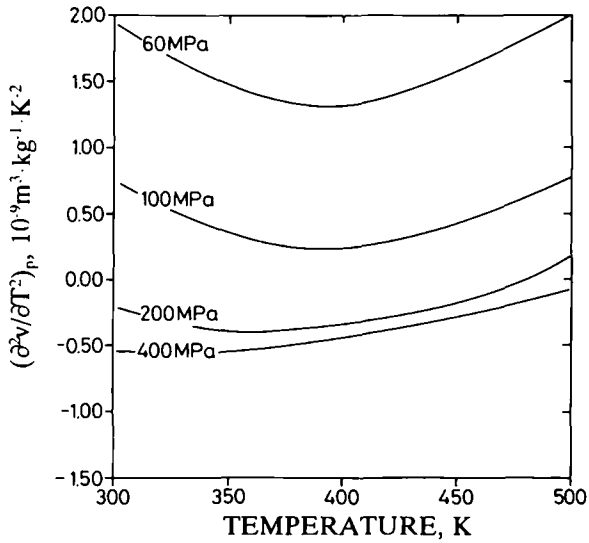

Fig. 7. Second derivative of the specific volume of *n*-hexane against temperature at selected pressures.

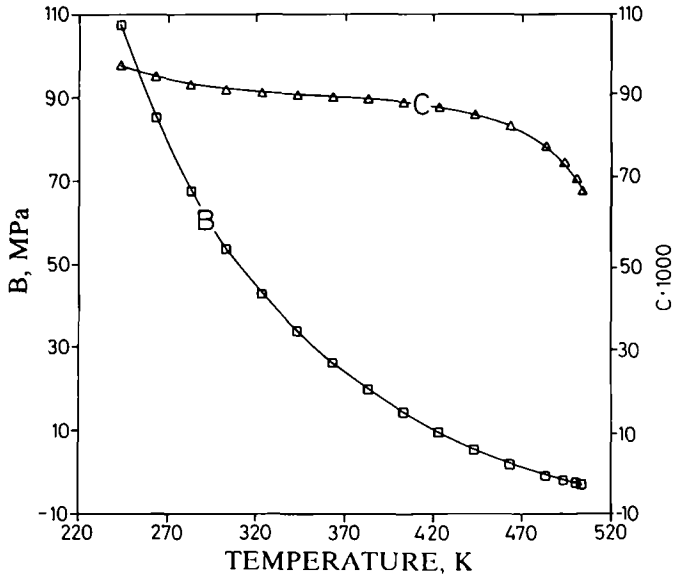

Fig. 8. Temperature dependences of parameters in the Tait equation for specific volumes of *n*-hexane.

Eq. (12) and as shown in Fig. 5. At low pressures, this pressure effect is large and negative and its magnitude increases rapidly with temperature, especially as the critical temperature is approached. At high pressures, the influence of pressure on C_p is much less. As a result the isotherms of C_p demonstrate a minimum. The pressure at which the minimum appears is shifted to higher values and the minima become flatter as temperature increases. This pressure effect on the isobaric specific heat capacity is also exhibited in the shape of the isobars. At pressures below the minimum on the isotherms the isobars diverge as the temperature increases (see Fig. 9A). However, at high pressures the isobars converge and cross at high temperatures (see Fig. 9B). The reason for this behavior can be found in Fig. 5B, which shows that the effect of pressure on the C_p of *n*-hexane at 503.15 K is practically nil above 200 MPa. Under these conditions C_p is independent of pressure and the isobars must meet.

The influence of pressure on the isochoric specific heat capacity C_v is also interesting. It has been reported [4] that C_v always increases with increasing pressure. However, the results of this study show that C_v does not always increase with pressure. Above 403.15 K a minimum appears in the isotherms of the pressure effect on C_v (Fig. 6). To check the accuracy of this observation, C_v was calculated for liquid argon from the pVT

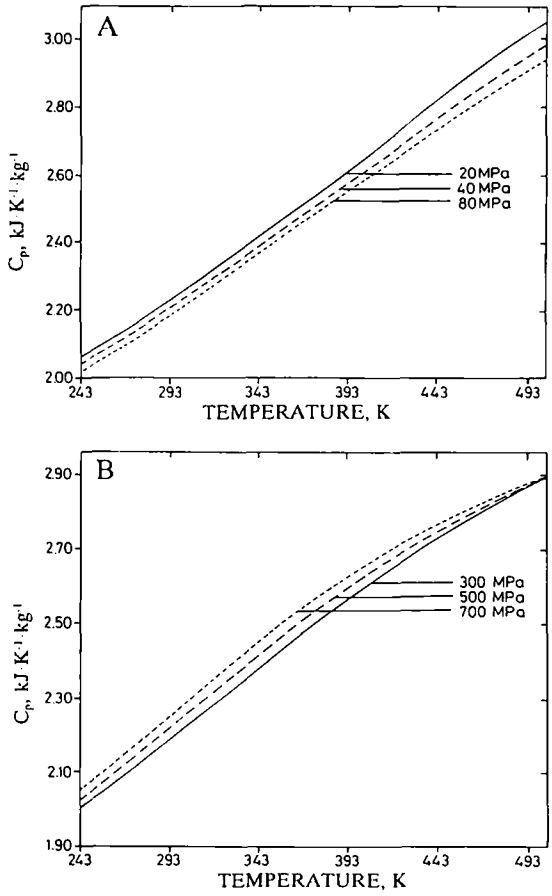

Fig. 9. Isobars of the specific isobaric heat capacity (C_p) of *n*-hexane at low pressures (A) and at high pressures (B).

equation of state and sound velocity data [49]. The results of these calculations, shown in Fig. 10, show that over similar temperature ranges with respect to the critical temperatures, the shapes of C_v isotherms for liquid argon are similar to those obtained for *n*-hexane in this study.

The difference $C_p - C_v$ can be derived directly from the equation of state; see Eq. (15). If there were no minima in the C_v isotherms, it could be argued that the minima in the C_p isotherms are a consequence of the pVT relations. The existence of minima in both the C_p and the C_v isotherms must result from a property not deducible from the pVT equation of state, for example, the influence of pressure on the intramolecular vibrational component of the heat capacity.

The specific heat capacities of *n*-hexane calculated in this paper can be compared with results of direct calorimetric measurements. Figure 11 presents, as solid lines, the isotherms of isobaric specific heat capacity at 303.15, 403.15, and 503.15 K calculated in the present study and, as discrete points, literature data [50] obtained by high-pressure flow calorimetry. The agreement is within the error of the two techniques, i.e., 1 to 2%. Figure 12 presents isotherms of both C_p and C_v at 298.15 K obtained in this study and literature data [44] obtained in a high-pressure calorimeter. The literature data fall between the isobaric and the isochoric heat capacities. Analysis of the construction of the calorimeter and the method of measurement as described in Ref. 44 explains why the measured heat capacity is neither C_p nor C_v. The pressure in the calorimeter was established at the beginning of the measurement and not corrected for changes caused by heating during the heat capacity measurements. The measurement was thus not done at constant pressure. The system was closed, but the measurement cannot be considered as a constant volume measurement because the calorimetric vessel was connected hydraulically to the pressure pump and the pressure changes caused by heating were partially compensated by compression of the hydraulic fluid. Thus the results of these

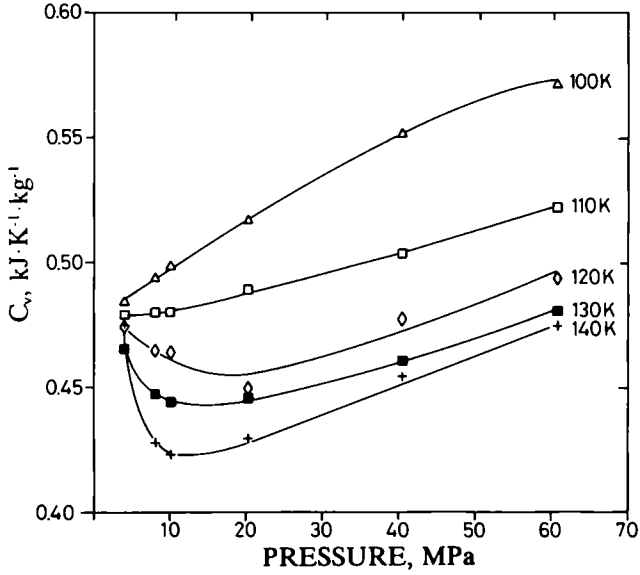

Fig. 10. Isochoric heat capacity of liquid argon at selected pressures and temperatures as calculated from data in Ref. 49. The lines shown aid in distinguishing the isotherms but should not be taken as numerically accurate representations.

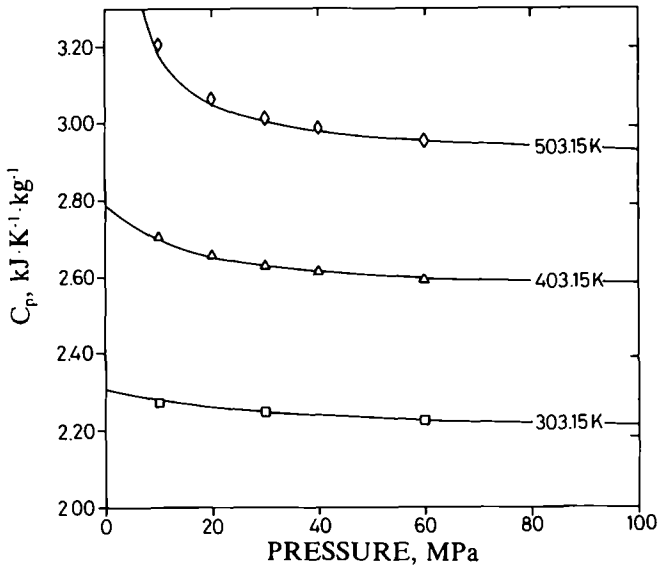

Fig. 11. Comparison of specific isobaric heat capacity determinations from the present study (lines) with flow calorimetric measurements (points) from Ref. 50.

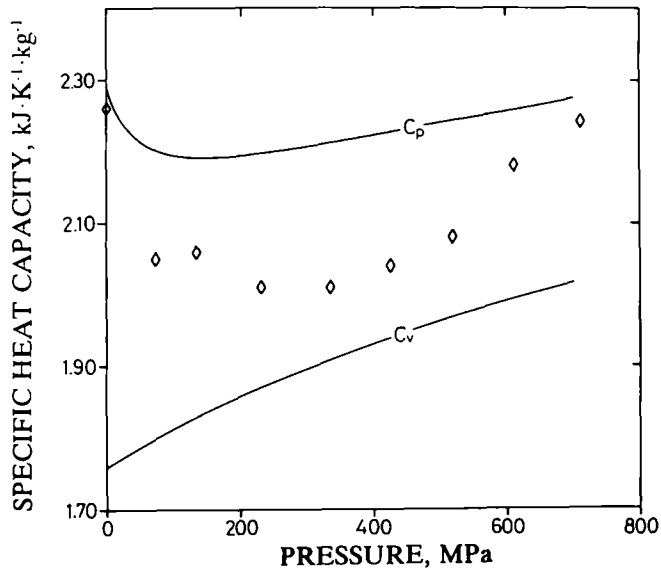

Fig. 12. Comparison of specific heat capacities at 298.15 K from the present study (lines) and determined with high-pressure calorimetric measurements (points) as described in Ref. 44.

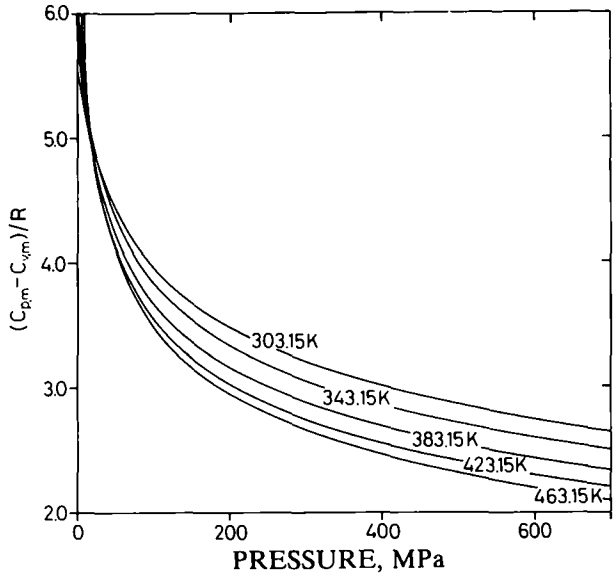

Fig. 13. Isotherms of the difference between isobaric and isochoric molar heat capacities of *n*-hexane.

measurements must fall somewhere between constant-volume and constant-pressure conditions as indicated in Fig. 12.

Another interesting feature of the results obtained in this study is the behavior of the difference between isobaric and isochoric heat capacities. Figure 13 shows that isotherms of this difference cross at 20 MPa. At this pressure the value of $C_{p,m} - C_{v,m}$ for *n*-hexane is $5R$ and is independent of temperature. This behavior results from the crossing of the isotherms of α_p and the lack of crossing of isotherms of κ_T [see Eq. (15)]. Molecular interpretation of this observation awaits further studies.

5. CONCLUSIONS

The results of measurements and calculations of various thermodynamic properties of *n*-hexane over the temperature range from 243.15 to 503.15 K under pressures from the saturation line up to 700 MPa presented in this paper lead to the following conclusions. (i) Isotherms of the coefficient of isobaric thermal expansivity, α_p, cross at 65 ± 2 MPa. Below this pressure α_p increases with temperature, but at higher pressures α_p decreases with temperature. At 65 ± 2 MPa, $\alpha_p = (8.95 \pm 0.09) \times 10^{-4}\ \mathrm{K}^{-1}$ and is independent of temperature. Over the entire range of pressure and temperature studied, α_p decreases with pressure. (ii) The specific volume

increases with temperature over the entire range of pressure and temperature studied. However, the isobars of specific volume are concave upward at low pressures and convex at high pressures. (iii) Isotherms of κ_T and $(\partial p/dT)_v$ do not cross on the whole pressure–temperature surface studied. (iv) The pressure effect on the isobaric specific heat capacity is negative at low pressure, increases rapidly with pressure at low pressure, becomes constant, and then decreases with pressure at high pressures. The isotherms of the pressure effect on C_p appear never to cross, but this observation must be verified for temperatures below 303.15 K. As a result of the pressure effect, isotherms of the isobaric heat capacity have a minimum that becomes flatter and shifts to higher pressures with increasing temperature. Isobars of C_p at pressures below the minimum in the C_p isotherms are concave upward or linear but convex at higher pressures and show a tendency to meet or cross at temperatures near the critical temperature. (v) The pressure effect on the isochoric specific heat capacity is always positive below 403.15 K but becomes negative above this temperature. The negative pressure effect increases with pressure up to about 15–30 MPa, depending on temperature, and then decreases. At temperatures above 463.15 K, the pressure effect on C_v is negative over the whole pressure range studied. As a result, isotherms of the isochoric specific heat capacity above 403.15 K have a minimum at relatively low pressures, i.e., 15–30 MPa. (vi) Isotherms of the difference $C_{p,m} - C_{v,m}$ demonstrate a crossing point at 20 ± 1 MPa. At this pressure $C_{p,m} - C_{v,m} = 5R$ and is independent of temperature. The difference increases with temperature at lower pressures and decreases with temperature at higher pressures. The difference decreases with increasing pressure over the whole temperature range.

The behavior of the thermodynamic properties of liquid *n*-hexane as functions of pressure and temperature can be used as a model for the behavior of other liquids without strong intermolecular interactions. The values of the thermodynamic parameters will be different for other liquids, but the general behavior on the p, T surface should be similar. Also, the equations and data given in this paper make *n*-hexane a more useful test and intercomparison substance for calibration and testing of high-pressure, high-temperature instruments and methods.

ACKNOWLEDGMENTS

This work was carried out partly in the frame of the Polish–French scientific cooperation program. S.L.R. wishes to express appreciation for the hospitality and financial support received from the Department of Chemistry, Brigham Young University, during his visits there.

REFERENCES

1. S. L. Randzio, in *Experimental Thermodynamics, Vol. IV, Solution Calorimetry*, K. N. Marsh and P. A. G. O'Hare, eds. (Blackwell Scientific, Oxford, in press) (1994).
2. Ph. Pruzan, *J. Phys. Lett.* **45**:273 (1984).
3. S. L. Randzio, *Thermochim. Acta* **121**:463 (1987).
4. Ph. Pruzan, *J. Chem. Thermodynam.* **234**:247 (1991).
5. B. A. Grigoryev, Y. L. Rastorguyev, A. A. Gerasimov, D. S. Kurumov, and S. A. Plotnikov, *Int. J. Thermophys.* **9**:439 (1988).
6. Tables of standard reference data *n*-hexane. *Thermodynamic Properties in the Ranges 180...630 K and 0.1...100 MPa*, GSSSD 90-85 (USSR State Committee on Standards, Moscow, 1986) (in Russian).
7. S. L. Randzio, D. J. Eatough, E.A. Lewis, and L. D. Hansen, *J. Chem. Thermodynam.* **20**:937 (1988).
8. G. L. Thomas and S. Young, *J. Chem. Soc.* **67**:1071 (1885).
9. L. B. Willingham, W. J. Taylor, J. M. Pignocco, and F. D. Rossini, *J. Res. Natl. Bur. Stand.* **35**:219 (1945).
10. D. E. Stewart, B. H. Sage, and W. N. Lacey, *Ind. Eng. Chem.* **46**:2529 (1954).
11. W. B. Nichols, H. H. Reamer, and B. H. Sage, *AIChE J.* **3**:262 (1957).
12. S. B. Kay, *J. Chem. Eng. Data* **16**:137 (1971).
13. S. A. Wieczorek and J. Stecki, *J. Chem. Thermodynam.* **10**:177 (1978).
14. H. Wolff and A. Shadiyakhy, *Fluid Phase Equil.* **7**:309 (1981).
15. R. A. Orwoll and P. J. Flory, *J. Am. Chem. Soc.* **89**:6814 (1967).
16. Y. L. Rastorguyev, B. A. Grigoryev, and D. S. Kurumov, *Izvest. Vysshikh Ucheb. Zavedenii Neft i Gaz* **11**:61 (1976).
17. D. S. Kurumov and B. A. Grigoryev, *Zhurn. Phyz. Khim.* **56**:551 (1982).
18. P. W. Bridgman, *Proc. Am. Acad. Arts. Sci.* **66**:185 (1931).
19. H. E. Eduljee, D. M. Newitt, and K. Weale, *J. Chem. Soc.* **4**:3086 (1951).
20. E. Kuss and M. Taslimi, *Chem. Ing. Techn.* **42**:1073 (1970).
21. R. Ta'ani, Dissertation (Universität Karlsruhe, Karlsruhe, 1976).
22. J. H. Dymond, K. J. Young, and J. D. Isdale, *J. Chem. Thermodynam.* **11**:887 (1979).
23. P. G. Tait, *I. Report on Some of the Physical Properties of Fresh Water and of Sea Water, The Report on the Scientific Results of the Voyage of the H.M.S. Challenger*, Physics and Chemistry, Vol. II, Part IV, 1888.
24. R. Ginell, *J. Chem. Phys.* **35**:1776 (1961).
25. V. Ruzicka, M. Zabransky, and V. Majer, *J. Phys. Chem. Ref. Data* **20**:405 (1991).
26. G. S. Parks and H. M. Huffman, *J. Am. Chem. Soc.* **52**:4381 (1930).
27. H. M. Huffman, G. S. Parks, and M. Barmore, *J. Am. Chem. Soc.* **53**:2705 (1931).
28. D. R. Stull, *J. Am. Chem. Soc.* **59**:2726 (1937).
29. N. M. Philip, *Proc. Indian Acad. Sci. Sect. A* **9**:109 (1939).
30. D. R. Douslin and H. M. Huffman, *J. Am. Chem. Soc.* **68**:1704 (1946).
31. T. J. Connolly, B. H. Sage, and W. N., Lacey, *Ind. Eng. Chem.* **43**:946 (1951).
32. E. Wilhelm, E. Rott, and F. Kohler, *Proc. 1st Int. Conf. Calor. Thermodynam.* (PWN, Warsaw, 1969), pp. 767–771.
33. W. M. Recko, K. W. Sadowska, and M. K. Woycicka, *Bull. Acad. Pol. Sci. Ser. Sci. Chim.* **19**:475 (1971).
34. M. Diaz Pena and J. A. R. Renuncio, *An. Quim.* **70**:113 (1974).
35. B. A. Grigoriev, Y. L. Rastorguyev, and G. S. Yanin, *Izvest. Vyssikh Uchebn. Zavedenii Neft i Gaz* **18**:63 (1975).
36. M. H. Karbalai Ghassemi and J.-P. E. Grolier, *Int. Data Ser. Sel. Data Mix. A* **95**:2 (1976).

37. B. Kalinowska, J. Jedlinska, W. Woycicki, and J. Stecki, *J. Chem. Thermodynam.* **12**:891 (1980).
38. J.-P. E. Grolier, A. Inglese, A. Roux, and E. Wilhelm, *Ber. Bunsenges. Phys. Chem.* **85**:768 (1981).
39. E. Wilhelm, A. Inglese, J. R. Quint, and J.-P. E. Grolier, *J. Chem. Thermodynam.* **14**:303 (1982).
40. G. C. Benson, P. J. D'Arcy, and M. K. Kumaran, *Thermochim. Acta* **75**:353 (1984).
41. R. Bravo, M. Pintos, M. C. Baluja, M. J. Paz Andrade, G. Roux-Desgranges, and J.-P. E. Grolier, *J. Chem. Thermodynam.* **16**:73 (1984).
42. M. Costas and D. Patterson, *Int. Data Ser. Sel. Data Mix. A* **212**:3 (1985).
43. M. Costas and D. Patterson, *J. Chem. Soc. Faraday Trans. I* **81**:635 (1985).
44. I. Czarnota, *High Temp.-High Press.* **17**:543 (1985).
45. G. C. Benson and P. J. D'Arcy, *Can. J. Chem.* **64**:2109 (1986).
46. B. A. Grigoryev and R. A. Andolenko, *Izvest. Vysshikh Uchebn. Zavedenii Neft i Gaz* **27**:60 (1984).
47. A. A. Gerasimov, *Izvest. Vysshikh Uchebn. Zavedenii Neft i Gaz* **23**:61 (1980).
48. S. L. Randzio, *Phys. Lett. A* **117**:1473 (1986).
49. W. B. Street, *Physica* **76**:59 (1974).
50. A. A. Gerasimov and B. A. Grigoriev, *Izvest. Vysshikh Uchebn. Zavedenii Neft i Gaz* **21**:46 (1978).